Submitted to

32nd International Conference on High Energy Physics, ICHEP04, Aug. 16-22, 2004, Beijing

Abstract: **12-0767**

Parallel Session **12**

www-h1.desy.de/h1/www/publications/conf/conf_list.html

Search for Doubly-Charged Higgs Production at HERA

H1 Collaboration

Abstract

A search for the single production of doubly-charged Higgs bosons $H^{\pm\pm}_{L,R}$ is performed in the framework of models in which a Higgs triplet is coupled to leptons of the i^{th} and j^{th} generation via Yukawa couplings $h^{L,R}_{ij}$. The signal is searched for via the decays of the doubly-charged Higgs to like-sign electron, muon, or tau pairs or electron-muon pairs, using a sample of $e^{\pm}p$ events corresponding to up to 118 pb^{-1} of data collected with the H1 detector at HERA for the ee, $\mu\mu$, μe channels and 65 pb^{-1} for the $\tau\tau$ channel. We observe no evidence for doubly-charged Higgs production and derive limits on the $h^{L,R}_{ee}$ and $h^{L,R}_{e\mu}$ Yukawa couplings as a function of the $H^{\pm\pm}_{L,R}$ mass. Assuming that the doubly-charged Higgs only decays to electrons, we set a lower limit of about 139 GeV on the $H^{\pm\pm}_{L,R}$ mass for a value $h^{L,R}_{ee} = 0.3$ corresponding to a coupling of electromagnetic strength. Assuming that the doubly-charged Higgs only decays to electron-muon, we set a lower limit of about 140 GeV on the $H^{\pm\pm}_{L,R}$ mass for a coupling value $h^{L,R}_{e\mu} = 0.3$.

1 Introduction

The H1 Collaboration has observed [1,2] multi-electron and multi-muon production at high transverse momentum in ep collisions at HERA. Six events are observed with a di-electron mass above 100 GeV, a domain where the Standard Model (SM) prediction is low. One di-muon event is found in the same mass region.

Based on these analyses, a search for the single production of doubly-charged Higgs bosons ($H^{\pm\pm}$), which may lead to high mass multi-lepton events, is presented in this paper. In the mass range covered by this analysis, the decay mode of the doubly-charged Higgs boson into a pair of like-sign charged leptons is expected to be dominant. Other decay modes are considered to be either theoretically suppressed or kinematically forbidden. The signal is searched for in ee, eee, $\mu\mu$, $e\mu$, $e\mu\mu$ and $\tau\tau$ final states. The ee, eee, $\mu\mu$, $e\mu$, and $e\mu\mu$ analyses make use of all data collected from 1994 to 2000 corresponding to an integrated luminosity up to 118 pb^{-1}. The $\tau\tau$ analysis makes use of the 1999–2000 data corresponding to an integrated luminosity of 65 pb^{-1}. This is the first search for doubly-charged Higgs production at HERA.

2 Phenomenology

Doubly-charged Higgs bosons appear in various extensions of the Standard Model, in which the usual Higgs sector is extended by one or more triplet(s) with non-zero hypercharge [3–5]. Examples are provided by some Left-Right Symmetric (LRS) models [6, 7], where the extended symmetry $SU(2)_L \times SU(2)_R \times U(1)_{B-L}$ is spontaneously broken to the SM symmetry $SU(2)_L \times U(1)_Y$ by an $SU(2)_R$ triplet of scalar fields, whose neutral component acquires a non-vanishing vacuum expectation value (vev). The Higgs triplet or triplets may be coupled to matter fields via Yukawa couplings. Whereas all charged fermions acquire their masses via their couplings to Higgs doublet(s), the vev of the neutral component of a Higgs triplet can give a Majorana mass to neutrinos, which is of particular interest since the existence of non-zero neutrino masses is suggested by recent experimental data.

At the tree level, doubly-charged Higgs bosons couple only to charged leptons and to other Higgs and gauge bosons. Couplings to quark pairs are not allowed by charge conservation. Although doubly-charged Higgs bosons may arise in various extensions of the SM, their couplings to charged leptons can be generically described by the Lagrangian:

$$\mathcal{L} = h_{ij}^{L,R} H^{--} \bar{l}_i^{\,c} P_{L,R} l_j \qquad + \text{ h.c.} \tag{1}$$

where $i, j = e, \mu, \tau$ are the generation indices, $P_{L,R} = (1 \mp \gamma^5)/2$, l are the charged lepton fields, and the superscript ^{c} denotes the charge conjugate spinors. The Yukawa couplings $h_{ij}^{L,R}$ are free parameters of the model. If the H^{--} field belongs to an $SU(2)_L$ triplet, H^{--} couples only to left-handed leptons; only the projector P_L and the couplings $h_{i,j}^L$ are then involved in equation (1). Models with an additional $SU(2)_R$ Higgs triplet contain an H^{--} field coupling to right-handed leptons via $h_{i,j}^R$. In the particular case of LRS models two doubly-charged Higgs bosons H_L^{--} and H_R^{--} are present, which couple to left-handed and right-handed leptons, respectively. Since the production processes at HERA I are insensitive to the chirality of the lepton fields[1], we consider here the generic case of a doubly-charged Higgs boson, which couples to either left-handed or right-handed leptons, and denote its Yukawa couplings by h_{ij} in the following.

For a non-vanishing coupling h_{ee} or h_{el} the single production of a doubly-charged Higgs boson is possible in $e\gamma^*$ interactions via the diagrams shown in Fig.1, where a photon is radiated by the proton or one of its constituent quarks[2]. The proton may be broken or remain intact during this interaction, leading to an inelastic or elastic reaction, respectively. The phenomenology of doubly-charged Higgs production at HERA was first discussed in Ref. [8], in which only the elastic channel was considered.

When only diagonal couplings h_{ii} are present in equation (1), the production process $e^{\pm}p \rightarrow e^{\mp}H^{\pm\pm}X$ is followed by the decays $H^{\pm\pm} \rightarrow e^{\pm}e^{\pm}(\mu^{\pm}\mu^{\pm}, \tau^{\pm}\tau^{\pm})$. Non-diagonal couplings (h_{ij} with $i \neq j$) would allow e.g. $e^{\pm}p \rightarrow \mu^{\mp}H^{\pm\pm}X$ followed by the decays $H^{\pm\pm} \rightarrow e^{\pm}\mu^{\pm}$ ($e^{\pm}\tau^{\pm}$, $\mu^{\pm}\tau^{\pm}$).

The indirect constraints [9–12] on doubly-charged Higgs can be parameterized in terms of the Higgs mass M_H and the Higgs couplings to leptons. The off-diagonal products $h_{ij}h_{i'j'}$ with either $i \neq j$ or $i' \neq j'$ suffer from stringent constraints for the first and second generation charged leptons from bounds on $\mu \rightarrow e^+e^-e^-$ and $\mu \rightarrow e\gamma$ decays [12]. Constraints on purely diagonal couplings or off-diagonal products $h_{ij}h_{ij}$ are less stringent. They come from the possible contribution of virtual $H^{\pm\pm}$ exchange to Bhabha scattering in e^+e^- collisions from PEP and PETRA which yield [9] $h_{ee} \leq 3.1 \times 10^{-3}\mathrm{GeV}^{-1}M_H$, using e^+e^- data taken at centre-of-mass energies of ~ 30 GeV. OPAL sets significantly more stringent limits on h_{ee} using data at centre-of-mass energies of $183 - 209$ GeV [13]. Search for muonium (μ^+e^-) to anti-muonium (μ^-e^+) conversion [9,12] yields $\sqrt{h_{ee}h_{\mu\mu}} \leq 7.6 \times 10^{-3}\mathrm{GeV}^{-1}M_H$. For the coupling $h_{\mu\mu}$ alone, avoiding possible extra contributions to $(g-2)_{\mu}$, yields $h_{\mu\mu} \leq 5 \times 10^{-3}\mathrm{GeV}^{-1}M_H$.

Previous direct searches for $H^{\pm\pm}$ pair production have been performed by the LEP and Tevatron experiments. For pair production in e^+e^- collisions, the kinematic reach is restricted to $M_H < \sqrt{s}/2$. Masses below approximately 100 GeV have been excluded by the DELPHI, L3, and OPAL experiments [14] in searches for $H^{\pm\pm}$ pair production at centre-of-mass energies between 189 and 209 GeV for any relative values of the h_{ee}, $h_{\mu\mu}$ and $h_{\tau\tau}$ couplings assuming a 100% decay branching fraction into charged leptons pairs. CDF [15] and DØ [16] performed searches for $H^{\pm\pm}$ pair production and CDF sets lower mass limits on the doubly charged Higgs decaying with a 100% branching fraction to ee ($100 < M_{H_L} < 133$ GeV and $101 < M_{H_R} < 109$ GeV excluded), $\mu\mu$ ($M_{H_L} > 136$ GeV and $M_{H_R} > 113$ GeV), or $e\mu$ ($M_{H_L} > 115$ GeV). OPAL performed a search for the single production of doubly charged Higgs and sets limits on h_{ee}, $h_{\mu\mu}$ and $h_{\tau\tau}$ at the order of 0.05 or below for masses up to 160 GeV [13].

In this paper we consider scenarios with diagonal couplings and Higgs decays into electrons, muons or taus through the process $e^{\pm}p \rightarrow e^{\mp}H^{\pm\pm}X \rightarrow e^{\mp}l^{\pm}l^{\pm}X$ involving h_{ee} at the Higgs production vertex and h_{ll} at its decay vertex. We also consider the scenario in which the off-diagonal coupling $h_{e\mu}$ is involved at the production vertex and the decay of the Higgs through the process $e^{\pm}p \rightarrow \mu^{\mp}H^{\pm\pm}X \rightarrow \mu^{\mp}e^{\pm}\mu^{\pm}X$. This leads to final states with three leptons, two of them being of like-sign and together having large invariant mass. It should be noted that the final state lepton which does not come from the Higgs decay is often scattered in the direction of the incident proton and may be lost in the beam pipe.

[1]HERA I operated with longitudinally unpolarised beams.

[2]The contribution of Z exchange in the diagrams shown in Fig.1 can be safely neglected.

3 Simulation of the Signal and Standard Model Backgrounds

The simulation of the doubly-charged Higgs signal, as well as the calculation of the signal cross-section, is performed using the CompHEP [17] package to evaluate the (lowest order) squared amplitudes corresponding to the elastic and inelastic processes [3]. The differential cross-sections are integrated with the VEGAS [20] package.

The parton densities in the proton used to estimate the inelastic contribution to the cross-section are taken from the CTEQ4L [21] parameterization. They are evaluated at the scale $\sqrt{Q^2}$, where Q^2 denotes the negative squared momentum transfer at the hadronic vertex. The inelastic cross-section is calculated in the range $Q^2 > 4$ GeV^2 and the quasi-elastic contribution in the range $1 < Q^2 < 4$ GeV^2. At the generator level, the parton shower approach [22], relying on the DGLAP [23] evolution equations, is used to simulate QCD corrections in the initial and final states. The hadronization of colored particles is then performed via an interface to the PYTHIA [19] program.

For the elastic contribution, the $e^\pm p \to e^\mp H^{\pm\pm} p$ cross-section is calculated by adding explicitly the proton to the particle contents of CompHEP. The photon-proton-proton current is described by the electric and magnetic form factors G_E and G_M. The usual dipole fit

$$G_E(Q^2) \simeq G_M(Q^2)/\mu_p \simeq G_D(Q^2) \equiv (1 + Q^2/(0.71\ \mathrm{GeV}^2))^{-2}$$

is used, where $\mu_p = 2.973$ is the magnetic moment of the proton. Using a linear fit for G_E, which takes into account the experimentally observed [24] decrease of $\mu_p G_E/G_M$ with increasing Q^2, changes the elastic cross-section by less than $\sim 2\%$.

For a Yukawa coupling $h_{ee} = 0.3$, the sum of the elastic, quasi-elastic, and inelastic contributions leads to a cross-section of ~ 0.39 pb (~ 0.04 pb) for a Higgs mass of 100 GeV (150 GeV). The quasi-elastic (inelastic) contribution is found to be $\sim 1/2$ $(1/3)$ of the elastic contribution in the mass range $80 - 150$ GeV. The theoretical uncertainty on the obtained cross-section is $\sim 4\%$ in this mass range. This is obtained by assessing an uncertainty of $\pm 2\%$ on the ratio $G_M(Q^2)/G_D(Q^2)$ [25], and by varying the scale at which the parton densities are evaluated to calculate the inelastic contribution between $\sqrt{Q^2}/2$ and $2\sqrt{Q^2}$.

The dominant SM contributions involved in multi-lepton production at HERA come from the interaction of two photons radiated from the incident electron and proton. Among these, the Bethe-Heitler process, where a lepton is exchanged in the t- or u-channel, is dominant. The Cabibbo-Parisi process, which involves an e^+e^- interaction where one of the electrons comes from a photon radiated from the proton, contributes at high transverse momentum only. The Drell-Yan process was calculated in [26] and was found to be negligible. All these processes are simulated with the GRAPE Monte Carlo generator [27], which also takes into account contributions from Bremsstrahlung with subsequent photon conversion into a lepton pair and electroweak contributions like real Z production with decay to l^+l^-. For multi-muon production additional contributions are considered, using DIFFVM [28] for the Υ resonance, LPAIR [29, 30] for muons arising from $\gamma\gamma \to \tau\tau$ and AROMA [31] for muons stemming from semi-leptonic decays in open heavy quark production ($c\bar{c}$ and $b\bar{b}$).

[3] The CompHEP implementation of the doubly-charged Higgs Lagrangian was used in [18] to calculate $e^-\gamma \to e^+\mu^+\mu^-$ cross-sections.

Experimental backgrounds are also present for multi-electron production, i.e. processes where, in addition to the scattered electron, one or more final state particles may be misidentified as electrons. They come dominantly from Neutral Current Deep Inelastic Scattering (NC-DIS) and from elastic Compton scattering, where a jet or a photon is misidentified as an electron. These processes are simulated with the DJANGO [32] and WABGEN [33] generators.

Backgrounds from NC-DIS and photoproduction (γp) contribute to tau-tau final states if isolated hadrons with pencil-like jet topology are misidentified as tau candidates. The γp background is simulated using the PYTHIA generator [19].

All Monte Carlo samples are subject to a full simulation of the H1 detector which takes into account the effects of energy loss, multiple scattering and showering in the detector.

4 Analysis of the $H^{\pm\pm} \to e^{\pm}e^{\pm}$, $\mu^{\pm}\mu^{\pm}$ Decays

For the $e^{\pm}p \to e^{\mp}H^{\pm\pm}X \to e^{\mp}e^{\pm}e^{\pm}X$ ($e^{\mp}\mu^{\pm}\mu^{\pm}X$) analysis we use the full $e^{\pm}p$ dataset recorded by the H1 experiment in the period 1994–2000. For the electron (muon) final states, the total integrated luminosity of 115.2 (113.7) pb^{-1} is shared between 36.5 (42.8) pb^{-1} and 65.1 (60.8) pb^{-1} of $e^{+}p$ collisions recorded at centre-of-mass energies $\sqrt{s}$ of 300 GeV and 318 GeV, respectively, and 13.6 (10.1) pb^{-1} of $e^{-}p$ collisions recorded at $\sqrt{s} = 318$ GeV.

This analysis is based on the H1 measurements of multi-electron production at high transverse momentum [1] and of multi-muon production [2]. The main selection criteria are summarized below and in Table 1. The selection of multi-electron events requires two central electron[4] candidates ($20^{\circ} < \theta^{e} < 150^{\circ}$, where θ^{e} is the electron polar angle measured with respect to the proton beam direction) one of which must have a transverse momentum $P_T^{e1} > 10$ GeV and the second $P_T^{e2} > 5$ GeV. Additional electron candidates are selected in the region ($5^{\circ} < \theta^{e} < 175^{\circ}$) when their energy is above 5 GeV (10 GeV if $5^{\circ} < \theta^{e} < 20^{\circ}$). The selected events are classified as di-electron ("2e") in the case that only the two central electron candidates are visible, and tri-electron ("3e") in the case in which exactly one additional electron candidate is identified. The muon-pair selection requires two central muon candidates ($20^{\circ} < \theta^{\mu} < 150^{\circ}$), with the transverse momenta $P_T^{\mu 1} > 10$ GeV and $P_T^{\mu 2} > 5$ GeV. Additional electrons or muons are accepted. After this selection, we observe 108 (17) data events in the di-(tri-) electron final state, which is to be compared with 117.1 ± 8.6 (20.3 ± 2.1) from SM expectation, and 56 data events in the di-muon and di-muon-electron final states which is to be compared with 54.7 ± 5.7 from SM expectation. No event with three or more muons or with two muons and more than one electron is observed. The distributions of the invariant mass M_{12} of the two highest P_T electrons and of the two muons $M_{\mu\mu}$ are shown in Fig.2. Overall, good agreement is observed between data and the SM expectation. The SM expectation is largely dominated by $\gamma\gamma$ contributions. In the multi-electron analysis and for masses $M_{12} > 100$ GeV, three "2e" events and three "3e" events are observed, compared to SM expectation of 0.30 ± 0.04 and 0.23 ± 0.04, respectively. In the multi-muon analysis, one di-muon event is found with $M_{12} > 100$ GeV, while 0.08 ± 0.01 are expected.

[4]Unless otherwise stated, the term "electron" is used in this paper to describe generically electrons or positrons.

Further selection criteria are then applied, which are designed to maximize the sensitivity of the analysis to a possible $H^{\pm\pm}$ signal.

The charge measurement of the two leptons assigned to the Higgs candidate is exploited. In e^+p (e^-p) collision mode, where H^{++} (H^{--}) bosons could be produced, events in which at least one of the two leptons is reliably assigned a negative (positive) charge are rejected. The charge assignment requires that the curvature κ of the track associated to the lepton is measured with an error satisfying $\mid \kappa/\delta\kappa \mid > 2$. The distribution of the invariant mass M_{12} of the two highest P_T electrons after requiring the charge assignment is shown in Fig.2.

For a given hypothetical $H^{\pm\pm}$ mass M_H, we define M_{ll} to be the invariant mass of the two leptons (or, for "3e" events, the invariant dilepton mass which is closest to M_H). In the M_H range $80 - 150$ GeV, the resolution for M_{ee} varies from ~ 3 GeV to ~ 5 GeV, while the resolution $\sigma_{\mu\mu}$ for $M_{\mu\mu}$ varies from ~ 4 GeV to ~ 20 GeV. The selection of Higgs candidates of mass M_H requires M_{ll} to be within a mass window designed to maximize the signal significance, which is found to be $M_H \pm 10$ GeV ($M_H \pm 2\sigma_{\mu\mu}$) for a Higgs decaying into electrons (muons).

Finally, for the electron channel, the precise measurement of the electron transverse momenta is further exploited by applying an additional M_H-dependent cut on the sum of the P_T of the two electrons assigned to the decay products of the Higgs candidate. The lower bound is chosen to keep 95% of the signal and is optimized separately for the di- and tri-electron final states. It varies between ~ 45 GeV and ~ 120 GeV in the considered M_H range.

multi-electron	**multi-muon**
Preselection criteria	
$P_T^{e_1} > 10$ GeV $P_T^{e_2} > 5$ GeV $20^\circ < \theta^{e_1,e_2} < 150^\circ$	$P_T^{\mu_1} > 2$ GeV $P_T^{\mu_2} > 1.75$ GeV $20^\circ < \theta^{\mu_1,\mu_2} < 160^\circ$ $M_{\mu\mu} > 5$ GeV
Final selection cuts	
no "wrong sign" lepton from $H^{\pm\pm}$ decay	
$\mid M_{ee} - M_H \mid < 10$ GeV large $P_T^{e_1} + P_T^{e_2}$	$\mid M_{\mu\mu} - M_H \mid < 2\sigma_{\mu\mu}$

Table 1: Selection criteria for the multi-electron and multi-muon Higgs decay channels.

Table 1 summarizes the selection criteria for both the multi-electron and the multi-muon analyses. After these requirements, the efficiency for selecting signal events varies from ~ 50 (35)% for an $H^{\pm\pm}$ mass of 80 GeV to ~ 35 (15)% for an $H^{\pm\pm}$ mass of 150 GeV in the electron (muon) analysis. For the electron channel, about half of the selected signal events are classified as di-electron in the mass range considered. The numbers of observed and expected events which satisfy all the above criteria are given in Table 2 for three values of M_H, together with the signal efficiencies. The three high mass events observed in the "3e" sample (see Fig.2) do not fulfill the criteria on the sum of the P_T of the two leptons applied to select high mass Higgs candidates. Amongst the three high mass events observed in the "2e" sample, only one event (at $M_{ee} = 112.5 \pm 2.4$ GeV) satisfies the required condition on the lepton charges. The high mass di-muon event does not satisfy the charge requirement.

M_H (GeV)	electron analysis ("2e" + "3e")				muon analysis			
	N_{obs}	N_{bckg}	ε	N_{signal}	N_{obs}	N_{bckg}	ε	N_{signal}
100	0	0.29	0.48	6.78	0	0.05	0.36	4.96
120	1	0.12	0.44	2.58	0	0.03	0.29	1.67
150	0	0.02	0.36	0.56	0	0.02	0.17	0.25

Table 2: Number of observed (N_{obs}) and expected (N_{bckg}) events from the multi-electron and multi-muon analyses which satisfy all criteria designed to select Higgs candidates of mass M_H. The signal selection efficiencies ε are also shown, together with the number of signal events (N_{signal}) expected for a Yukawa coupling $h_{ee} = 0.3$.

For the multi-electron analysis, the theoretical and experimental systematic uncertainties attributed to the Monte Carlo predictions are detailed in [1]. The main contribution to the experimental systematic error on the signal and SM predictions is due to the tracker efficiency in the electron identification procedure, which is 90% on average with an uncertainty increasing with decreasing polar angle from 3% to 15%. Systematic errors due to the uncertainty on the electromagnetic energy scale (known at the 0.5 to 3% level in the central and forward regions of the detector, respectively) and to the trigger efficiency are also taken into account.

The dominant experimental systematic errors on the signal and SM expectation in the multi-muon analysis are due to the trigger efficiency ($\sim 70\%$ and $\sim 80\%$ for inelastic and elastic signal events respectively, with an uncertainty of about 6%), and to the uncertainty of the muon identification which was found to be 6%.

In both analyses the statistical error of the Monte Carlo samples is taken into account as an additional systematic error. Finally, the luminosity measurement leads to a normalization uncertainty of 1.5%. These theoretical and experimental systematic uncertainties added in quadrature lead to a total signal systematic error of about 11% (13%) for the multi-electron(-muon) analysis.

5 Analysis of the $H^{\pm\pm} \rightarrow e^{\pm}\mu^{\pm}$ Decay

The full $e^{\pm}p$ dataset of the run period 1994–2000 was used for the analysis of the process $e^{\pm}p \rightarrow \mu^{\mp}H^{\pm\pm}X \rightarrow \mu^{\mp}e^{\pm}\mu^{\pm}X$, and corresponds to a total integrated luminosity of 118 pb^{-1}.

The electron and muon identification criteria are the same as for the analysis of the $e^{\pm}e^{\pm}$ and $\mu^{\pm}\mu^{\pm}$ channels and are described in [1] and [2], respectively. Electrons are identified in the polar angle range 20° $< \theta^e <$ 140° and with a minimum transverse momentum of $P_T^e >$ 10 GeV, to ensure a high trigger efficiency of the events. Muons are required to have a momentum $P_T^{\mu} >$ 5 GeV and to be in the polar angle range 10° $< \theta^e <$ 140°. Events are selected with at least one electron and muon fulfilling the above criteria. Moreover an isolation distance of 0.5 in $\eta - \phi$ space is required between the two leptons. After this selection, 35 data events are observed compared to a SM expectation of 30.6 $\pm$ 2.8. The distribution of the invariant mass of the electron and the muon $M_{e\mu}$ is presented in Fig.2. Good agreement is observed between data and the SM expectation and no data events with $M_{e\mu} >$ 70 GeV are present.

Similar to the analysis of the $e^\pm e^\pm$ and $\mu^\pm\mu^\pm$ channels, further selection criteria are applied in order to maximise the sensitivity to an $H^{\pm\pm}$ signal. Events in which at least one of the two leptons is reliably assigned a negative (positive for e^-p data) charge are rejected. For events with two identified muons and one electron, we define $M_{e\mu}$ to be the electron-muon invariant mass which is closest to a given $H^{\pm\pm}$ mass M_H. The resolution $\sigma_{e\mu}$ on $M_{e\mu}$ varies from $\sim$ 4 GeV to $\sim$ 8 GeV in the M_H range 80–150 GeV. The selection of Higgs candidates of mass M_H further requires $M_{e\mu}$ to be within a mass window of $2\sigma_{e\mu}$. The resulting signal efficiency varies from $\sim$ 55% to $\sim$ 45% for M_H in the range 80–150 GeV. The numbers of observed and expected events which satisfy all the above criteria are given in Table 3 for three values of M_H, together with the signal efficiencies. The experimental systematic errors are similar to those given in the previous section.

M_H	**electron-muon analysis**			
(GeV)	N_{obs}	N_{bckg}	ε	N_{signal}
100	0	1.01	0.49	7.12
120	0	0.65	0.47	2.82
150	0	0.33	0.42	0.67

Table 3: Number of observed (N_{obs}) and expected events from the electron-muon analysis which satisfy all criteria designed to select Higgs candidates of mass M_H. The signal selection efficiencies ε are also shown, together with the number of signal events (N_{signal}) expected for a Yukawa coupling $h_{e\mu} = 0.3$.

6 Analysis of the $H^{\pm\pm} \to \tau^\pm\tau^\pm$ Decay

For the $e^+p \to e^-H^{++}X \to e^-\tau^+\tau^+X$ analysis we use the e^+p dataset recorded by the H1 experiment in the period 1999–2000 corresponding to a total integrated luminosity of 65.4 pb^{-1} at centre-of-mass energy of $\sqrt{s} = 318$ GeV.

The selection of $\tau\tau$ final states requires two high P_T tau candidates in the central region of the detector $20^\circ < \theta^\tau < 160^\circ$. The tau identification is based on charged tracks measured in the central jet chamber with a transverse momentum $P_T^{\tau 1} > 10$ GeV and $P_T^{\tau 2} > 5$ GeV. They have to be separated in the pseudorapidity-azimuth [5] plane by $R > 2.5$.

Candidate events are selected by requiring the longitudinal position of the primary interaction to be within 35 cm around the nominal interaction point and by applying topological filters to remove background induced by cosmic showers and other non-ep sources. The large background from NC-DIS at low Q^2 is reduced by rejecting events with an electromagnetic energy deposition in the backward SpaCal calorimeter of more than 5 GeV.

The leptonic tau decays $\tau \to e\nu\nu$ and $\tau \to \mu\nu\nu$ are reconstructed by identifying the decay electron in the LAr calorimeter or the muon in the central muon detector, respectively. Remaining tau candidates are reconstructed as hadronic tau decay if at least 40% of the charged track momentum is reconstructed in the LAr calorimeter. After this preselection about 24000 events

[5] $R = \sqrt{\Delta\eta^2 + \Delta\varphi^2}$, with $\Delta\eta$ being the distance in pseudorapidity

are found compared to 26000, mainly expected from NC-DIS. These events are classified in $e\mu$, ej, μj and jj candidate classes for further analysis.

Further selection criteria are applied to reduce mainly background due to misidentification of taus in γp and NC-DIS. Tau candidates are required to be isolated from other tracks in the event in a cone $0.15 < R < 1.5$ for hadronic decays and $R < 1.5$ for leptonic decays. In order to suppress background from NC-DIS which is peaked at small scattering angles, the polar angle of electrons is required to be below 120°. For the ej class, which suffers large backgrounds from NC-DIS, energy and longitudinal momentum invariance ($\sum_i E^i - P_z^i = 2E_e = 55$ GeV for all particles) measured from all visible particles is required to be smaller than 45 GeV to account for the missing tau neutrinos in the event. To reduce remaining background from γp and NC-DIS with large activity in the forward region of the calorimeter, no significant energy deposition is allowed in the jj and ej classes with $\eta > 2.8$.

Finally, the invariant mass of the tau-tau system $M_{\tau\tau}$ is fitted by imposing $\sum_i E^i - P_z^i \equiv 2E_e$, by assuming the missing neutrinos to be in the direction of the tau tracks and by minimising the missing transverse momentum in the event. The mass resolution of this fit is about 4 GeV in the Higgs mass range 80 to 150 GeV. The results after the $\tau\tau$ selection and for $M_{\tau\tau} > 65$ GeV are shown in Table 4. One event is selected with oppositely charged tracks and with a

Decay Topology	$\tau\tau$ **preselection**			$H^{\pm\pm}$ **final selection**			**Eff.**$\times$**BR**	
	obs.	SM bg	($\tau\tau$)	obs.	SM bg	($\tau\tau$)	elastic	quasi-elastic
$e\mu$	0	0.29± 0.03	(0.11)	0	0.09± 0.01	(0.00)	2.9%	2.6%
ej	0	1.20± 0.24	(0.31)	0	0.78± 0.16	(0.03)	6.9%	2.8%
μj	0	0.25± 0.05	(0.16)	0	0.03± 0.01	(0.03)	6.4%	5.5%
jj	1	0.38± 0.10	(0.16)	0	0.13± 0.08	(0.00)	8.0%	2.9%
total	1	2.12± 0.32	(0.74)	0	1.03± 0.19	(0.06)	24.2%	13.8%

Table 4: Number of observed and expected tau tau candidates after $\tau\tau$ selection and after the $H^{\pm\pm}$ selection requiring like-sign charges. The expectation is given for all SM processes and for the process $\gamma\gamma \to \tau\tau$. The efficiencies including the branching ratio of $\tau\tau \to \mathrm{class}_{ij}$, where i, j stands for e, μ, j, are given after final selection for the elastic and quasi-elastic production process for $M_H = 100$ GeV.

reconstructed invariant mass of 85 GeV in the jj class compared to a total SM expectation of 2.1 events (dominated by NC-DIS) and 0.7 events from $\gamma\gamma \to \tau^+\tau^-$.

In a final step, both charges of the τ candidates are required to be like-sign as expected for doubly charged Higgs bosons. This cut is only applied if both τ candidates have a 1-prong signature. It removes almost completely background from $\gamma\gamma \to \tau^+\tau^-$ and increases the purity in the $e\mu$ and ej classes where in some cases the scattered electron is wrongly selected as τ candidate.

The signal efficiencies depend only weakly on M_H. They are summarized for the elastic and quasi-elastic production process in Table 4 after applying the like-sign charge cut for a $H^{\pm\pm}$ mass of $M_H = 100$ GeV and include the branching ratios for the different decay classes. The main experimental systematic uncertainty of 6% is due to the track reconstruction efficiency. All systematic errors including uncertainties from the luminosity measurement, lepton and jet identification are added in quadrature and result in a total uncertainty of 10% for all classes.

Because of the smallness of the background expectation after applying all cuts, remaining background is ignored in the following statistical interpretation and no background subtraction is performed.

7 Interpretation

After the final Higgs selection criteria no significant excess over the SM expectation remains in the data. Upper limits on the signal cross-section and on the doubly-charged Higgs couplings $h_{ee}^{L,R}$ and $h_{e\mu}^{L,R}$ are derived as a function of the $H^{\pm\pm}$ mass at the 95% confidence level following a Bayesian approach [34] that takes statistical and systematic uncertainties into account. The limits at 95% confidence level on the product of the $H^{\pm\pm}$ production cross-section and the decay branching ratio, $\sigma(e^{\pm}p \rightarrow e^{\mp}H^{\pm\pm}X) \times \mathrm{BR}(H^{\pm\pm} \rightarrow l^{\pm}l'^{\pm})$, for the leptonic decays $H^{\pm\pm} \rightarrow e^{\pm}e^{\pm}$, $\mu^{\pm}\mu^{\pm}$, $\tau^{\pm}\tau^{\pm}$ and $e^{\pm}\mu^{\pm}$ are shown in Fig.3 as a function of the doubly-charged Higgs mass. The cross-section limits vary from 0.25 to 0.3 pb for the $\tau\tau$ channel and from 0.05 to 0.15 pb for the channels with decays into electrons and muons.

The bounds on $\sigma(e^{\pm}p \rightarrow e^{\mp}H^{\pm\pm}X) \times \mathrm{BR}(H^{\pm\pm} \rightarrow l^{\pm}l^{\pm})$ are interpreted in terms of mass-dependent upper limits on the couplings $h_{ee}^{L,R}$, $h_{\mu\mu}^{L,R}$, and $h_{\tau\tau}^{L,R}$. Assuming a democratic coupling of the doubly-charged Higgs to leptons, i.e. $\mathrm{BR}(H^{\pm\pm} \rightarrow l^{\pm}l^{\pm}) = 1/3$, the electron, muon, and tau channels and the combination of these three channels allow a mass-dependent upper limit on $h_{ee}^{L,R} = h_{\mu\mu}^{L,R} = h_{\tau\tau}^{L,R}$ shown in Fig.4. We set a lower limit on $M_{H_{L,R}}$ of about 108 (109) GeV in the electron (muon) channel for $h_{ll}^{L,R} = 0.3$, corresponding to an interaction of electromagnetic strength ($h_{ee}^2/4\pi \simeq \alpha_{em}$). The combination of the electron, muon and tau channels gives a lower limit on $M_{H_{L,R}}$ of 119 GeV for $h_{ll}^{L,R} = 0.3$.

The resulting constraints are also shown in Fig.5 assuming that the doubly-charged Higgs bosons only decay to electrons, i.e. $\mathrm{BR}(H^{\pm\pm} \rightarrow e^{\pm}e^{\pm}) = 1$. We set a lower limit on $M_{H_{L,R}}$ of about 139 GeV for $h_{ee}^{L,R} = 0.3$. The result is compared to indirect limits from Bhabha scattering from OPAL [13], to limits from direct searches for single production of doubly-charged Higgs from OPAL [13], and from pair production from CDF [15] and the LEP experiments [14].

From the $e^{\pm}p \rightarrow \mu^{\mp}H^{\pm\pm}X \rightarrow \mu^{\mp}e^{\pm}\mu^{\pm}X$ analysis we set upper limits on $h_{e\mu}^{L,R}$. Assuming that the doubly-charged Higgs bosons only decay to electron-muon, i.e. $\mathrm{BR}(H^{\pm\pm} \rightarrow e^{\pm}\mu^{\pm}) = 1$, we set a lower limit on $M_{H_{L,R}}$ of about 140 GeV for $h_{e\mu}^{L,R} = 0.3$. The results of this analysis are shown in Fig.6 and compared to limits from direct searches for pair production of doubly-charged Higgs from CDF [15] and the LEP experiments [14]. The H1 limits extend the excluded region in the electron-muon channel to masses that are beyond those reached in previous searches for pair production at LEP and the Tevatron.

8 Conclusion

We have presented a dedicated search for the single production of doubly-charged Higgs bosons, combining ee, eee, $\mu\mu$, $e\mu$, $e\mu\mu$ and $\tau\tau$ final states. In a previous model independent analysis, H1 observed six events with a di-electron mass above 100 GeV, a region where the Standard

Model expectation is small. Out of the six events, only one is compatible with the production of a doubly-charged Higgs boson when kinematic cuts and lepton charges are taken into account. No multi-muon, multi-tau, nor electron-muon event is found in this mass domain compatible with the production of a doubly-charged Higgs boson.

This analysis places new limits on the $H^{\pm\pm}$ mass and its Yukawa coupling to electrons and muons. Assuming that the doubly-charged Higgs only decays to electrons, we set a lower limit on $M_{H_{L,R}}$ of about 139 GeV for a coupling value $h_{ee}^{L,R} = 0.3$, corresponding to an interaction of electromagnetic strength. Assuming that the doubly-charged Higgs only decays to electron-muon, we set a lower limit on $M_{H_{L,R}}$ of about 140 GeV for a coupling value $h_{e\mu}^{L,R} = 0.3$.

Acknowledgements

We are grateful to the HERA machine group whose outstanding efforts have made this experiment possible. We thank the engineers and technicians for their work in constructing and maintaining the H1 detector, our funding agencies for financial support, the DESY technical staff for continual assistance and the DESY directorate for support and for the hospitality which they extend to the non DESY members of the collaboration.

We are specially grateful to J. Maalampi and N. Romanenko for providing the doubly-charged Higgs Lagrangian implementation in CompHEP which was used in this analysis. We would like also to thank K. Huitu, N. Romanenko and E. Boos for their help and valuable discussions.

References

[1] A. Aktas *et al.* [H1 Collaboration], Eur. Phys. J. C **31** (2003) 17 [hep-ex/0307015].

[2] A. Aktas *et al.* [H1 Collaboration], [hep-ex/0311015].

[3] G. B. Gelmini and M. Roncadelli, Phys. Lett. B **99** (1981) 411.

[4] J. C. Pati and A. Salam, Phys. Rev. D **10** (1974) 275; R. E. Marshak and R. N. Mohapatra, Phys. Lett. B **91** (1980) 222.

[5] R. N. Mohapatra and G. Senjanovic, Phys. Rev. Lett. **44** (1980) 912.

[6] G. Senjanovic and R. N. Mohapatra, Phys. Rev. D **12** (1975) 1502.

[7] R. N. Mohapatra and R. E. Marshak, Phys. Rev. Lett. **44** (1980) 1316 [Erratum-ibid. **44** (1980) 1643].

[8] E. Accomando and S. Petrarca, Phys. Lett. B **323** (1994) 212 [hep-ph/9401242].

[9] M. L. Swartz, Phys. Rev. D **40** (1989) 1521.

[10] J. F. Gunion, J. Grifols, A. Mendez, B. Kayser and F. I. Olness, Phys. Rev. D **40** (1989) 1546.

[11] M. Lusignoli and S. Petrarca, Phys. Lett. B **226** (1989) 397.

[12] G. Barenboim, K. Huitu, J. Maalampi and M. Raidal, Phys. Lett. B **394** (1997) 132 [hep-ph/9611362].

[13] G. Abbiendi *et al.* [OPAL Collaboration], Phys. Lett. B **577** (2003) 93 [hep-ex/0308052].

[14] J. Abdallah *et al.* [DELPHI Collaboration], Phys. Lett. B **552** (2003) 127 [hep-ex/0303026]; P. Achard *et al.* [L3 Collaboration], Phys. Lett. B **576** (2003) 18 [hep-ex/0309076]; G. Abbiendi *et al.* [OPAL Collaboration], Phys. Lett. B **526** (2002) 221 [hep-ex/0111059].

[15] D. Acosta *et al.* [CDF Collaboration], submitted to Phys. Rev. Lett [hep-ex/0406073].

[16] V. M. Abazov *et al.* [D0 Collaboration], submitted to Phys. Rev. Lett [hep-ex/0404015].

[17] E. E. Boos, M. N. Dubinin, V. A. Ilyin, A. E. Pukhov and V. I. Savrin [hep-ph/9503280]; E.E. Boos *et al.*, Proceedings of the Xth Int. Workshop on High Energy Physics and Quantum Field Theory, QFTHEP-95, (Moscow, 1995), Eds. B. Levtchenko and V. Savrin, p 101.

[18] S. Godfrey, P. Kalyniak and N. Romanenko, Phys. Rev. D **65** (2002) 033009 [hep-ph/0108258].

[19] T. Sjostrand, P. Eden, C. Friberg, L. Lonnblad, G. Miu, S. Mrenna and E. Norrbin, Comput. Phys. Commun. **135** (2001) 238 [hep-ph/0010017].

[20] G.P. Lepage (Cornell U., LNS), CLNS-80/447 (1980).

[21] H. L. Lai *et al.*, Phys. Rev. D **55** (1997) 1280 [hep-ph/9606399].

[22] JETSET 7.4: T. Sjöstrand, Lund Univ. preprint LU-TP-95-20 (August 1995) 321pp; *ibid.*, CERN preprint TH-7112-93 (February 1994) 305pp.

[23] V. N. Gribov and L. N. Lipatov, Yad. Fiz. **15** (1972) 781 [Sov. J. Nucl. Phys. **15** (1972) 438]; G. Altarelli and G. Parisi, Nucl. Phys. B **126** (1977) 298; Y. L. Dokshitzer, Sov. Phys. JETP **46** (1977) 641 [Zh. Eksp. Teor. Fiz. **73** (1977) 1216].

[24] O. Gayou *et al.* [Jefferson Lab Hall A Collaboration], Phys. Rev. Lett. **88** (2002) 092301 [nucl-ex/0111010].

[25] R. C. Walker *et al.*, Phys. Rev. D **49** (1994) 5671.

[26] N. Arteaga-Romero, C. Carimalo and P. Kessler, Z. Phys. C **52**, 289 (1991).

[27] T. Abe, Comput. Phys. Commun. **136** (2001) 126 [hep-ph/0012029].

[28] B. List, Diploma Thesis, Technische Universität Berlin, H1-10/93-319 (1993).

[29] S.P. Baranov, O. Dunger, H. Shooshtari and J.A. Vermaseren, Hamburg 1991, Proceedings, Physics at HERA, Vol. 3 pp. 1478-1482.

[30] J. A. M. Vermaseren, Nucl. Phys. B **229** (1983) 347.

[31] G. Ingelman, J. Rathsman and G. A. Schuler, Comput. Phys. Commun. **101** (1997) 135 [hep-ph/9605285].

[32] DJANGO 2.1: G.A. Schuler and H. Spiesberger, Proceedings of the Workshop Physics at HERA, Vol 3 p. 1419.

[33] Ch. Berger and P. Kandel, "A new Generator for Wide Angle Bremsstrahlung", Proc. of the Monte Carlo Generators for HERA Physics Workshop, DESY-PROC-1999-02, p. 596.

[34] R. M. Barnett *et al.* [Particle Data Group Collaboration], Phys. Rev. D **54** (1996) 1.

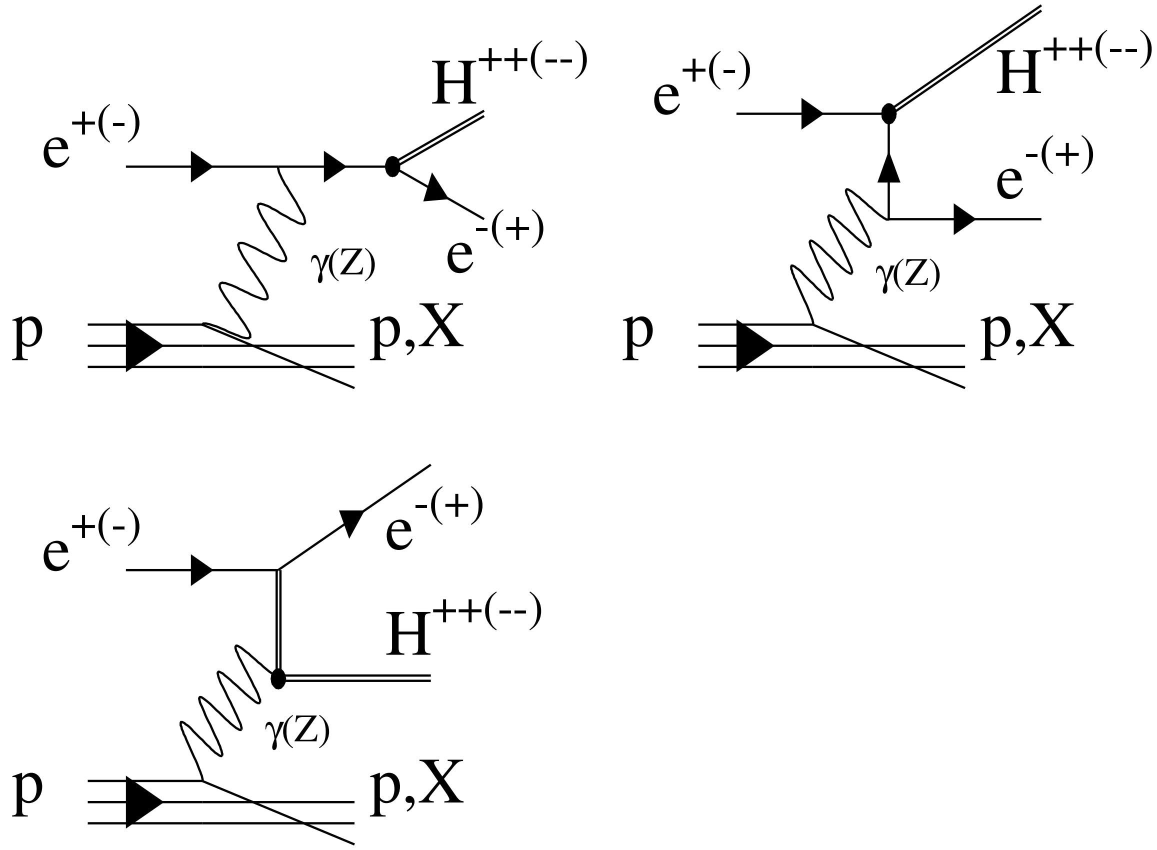

Figure 1: Feynman diagrams for the single production of doubly-charged Higgs bosons in $e^{\pm}p$ collisions at HERA involving the h_{ee} coupling at the production vertex and the decay of the Higgs. The hadronic final state is denoted by p (X) in the elastic (inelastic) case, where the initial proton remains intact (dissociates).

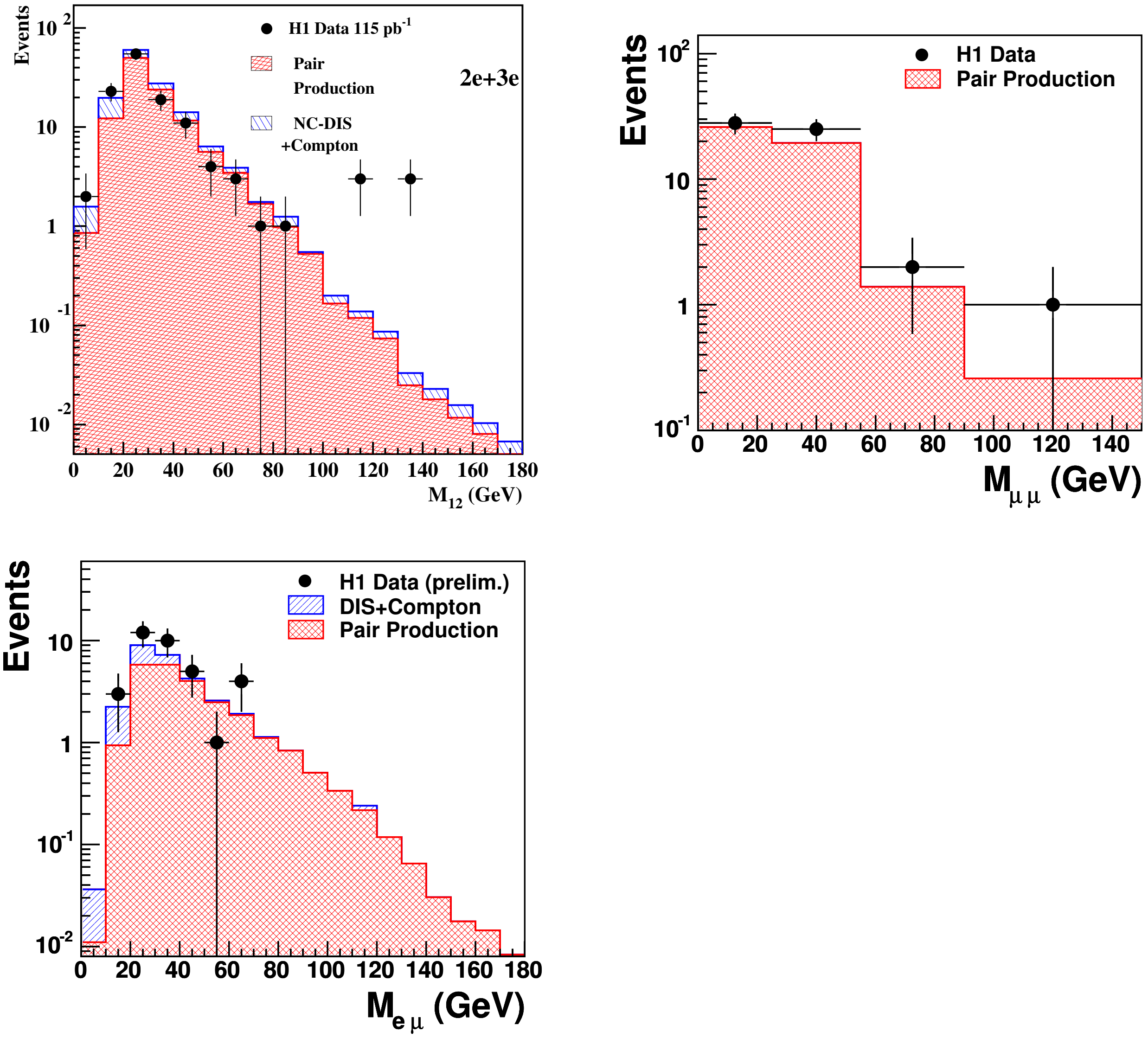

Figure 2: Invariant mass M_{12} of the two highest P_T electrons for events classified as di-electron and tri-electron (top left), di-muon invariant mass $M_{\mu\mu}$ (top right), and electron-muon invariant mass (bottom left), compared with the Standard Model expectation.

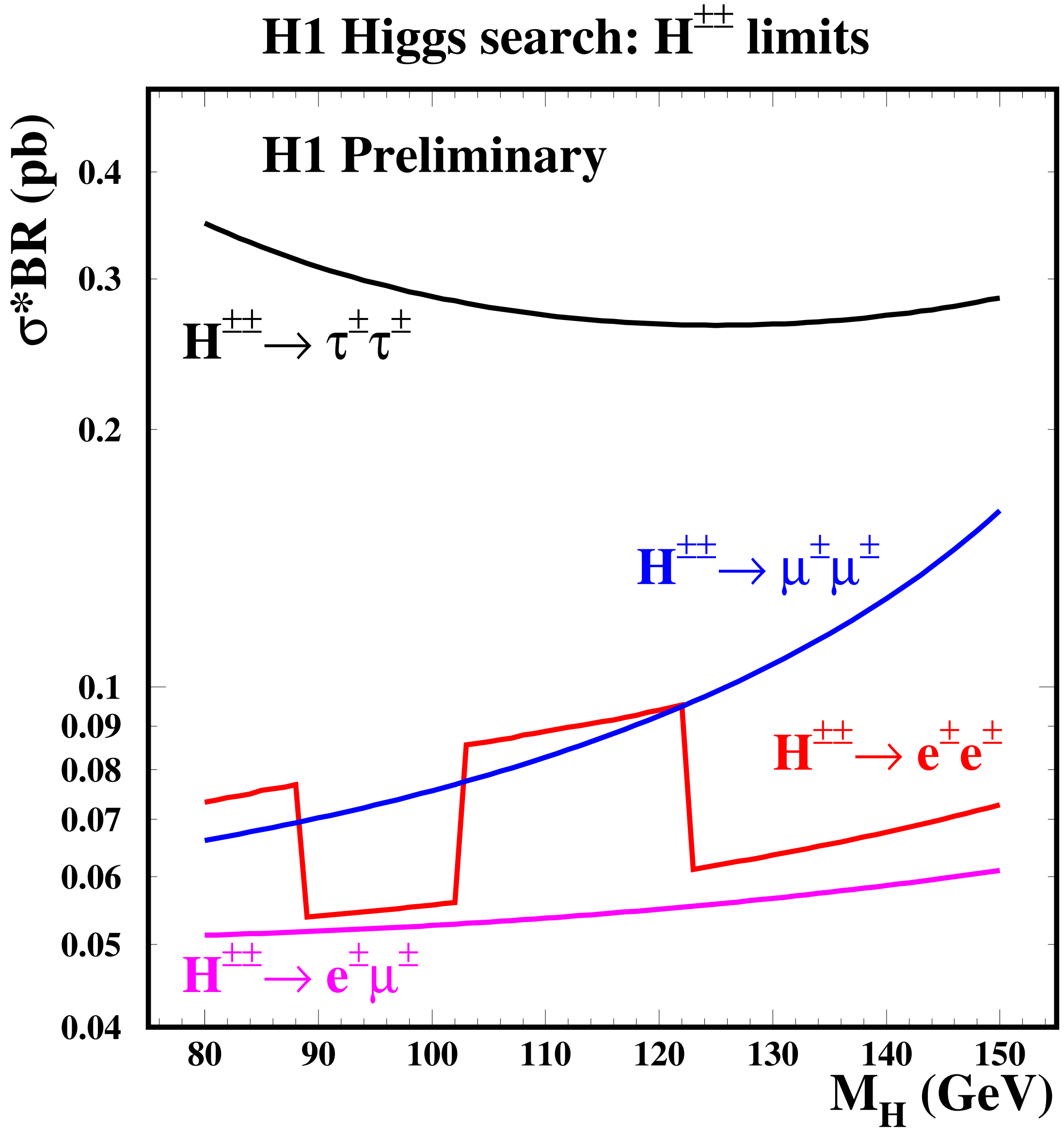

Figure 3: Upper limits at 95% confidence level on $\sigma(e^{\pm}p \rightarrow e^{\mp}H^{\pm\pm}X) \times \mathrm{BR}(H^{\pm\pm} \rightarrow l^{\pm}l'^{\pm})$ as a function of the doubly-charged Higgs mass.

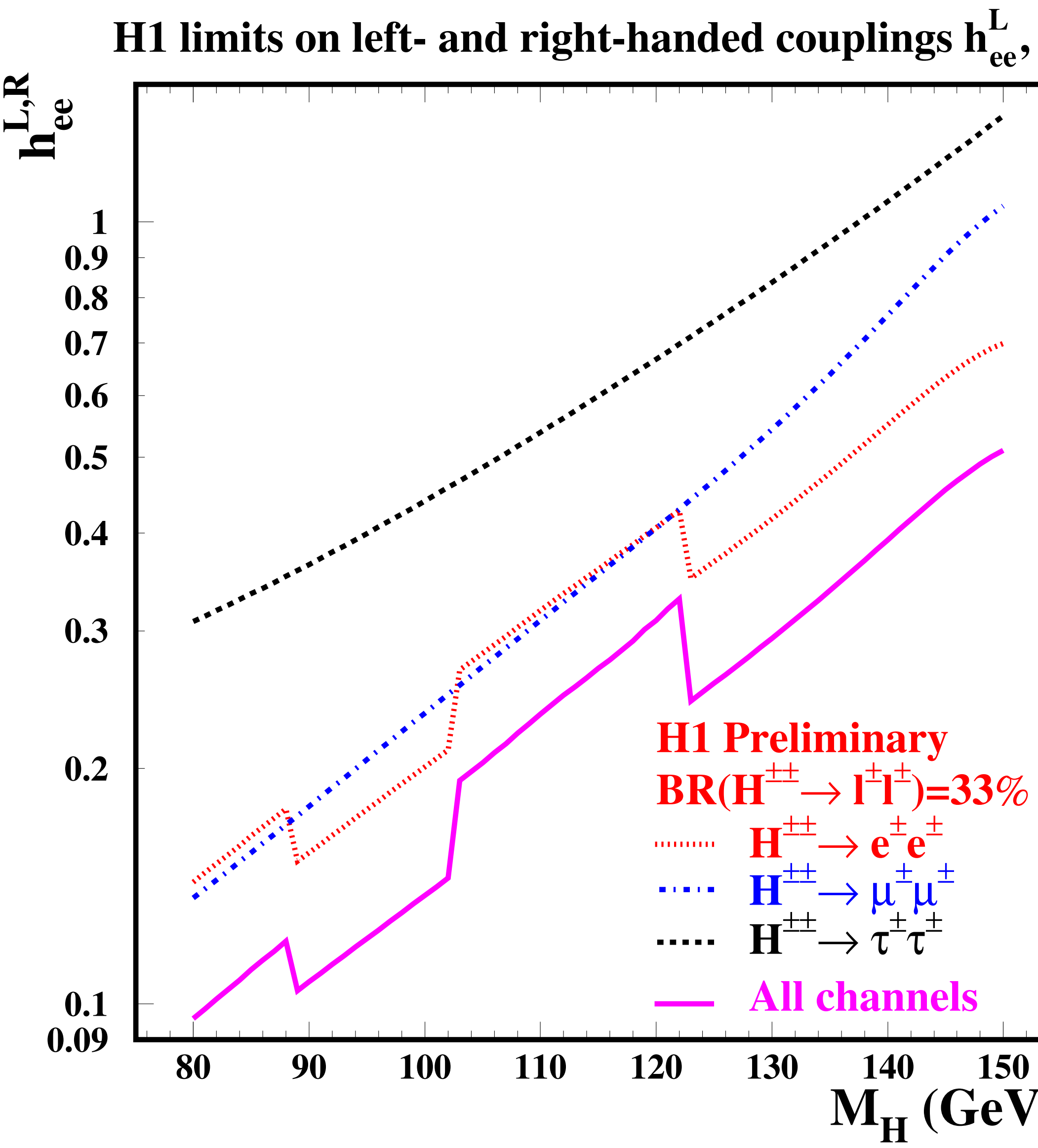

Figure 4: Exclusion limits on the coupling $h_{ee}^{L,R}$ at 95% confidence level as a function of the doubly-charged Higgs mass for the decay channels $H^{\pm\pm} \to e^{\pm}e^{\pm}, \mu^{\pm}\mu^{\pm}, \tau^{\pm}\tau^{\pm}$ and the combination of these channels (full curve), assuming a democratic coupling of the doubly-charged Higgs to leptons, i.e. BR$(H^{\pm\pm} \to l^{\pm}l^{\pm}) = 1/3$.

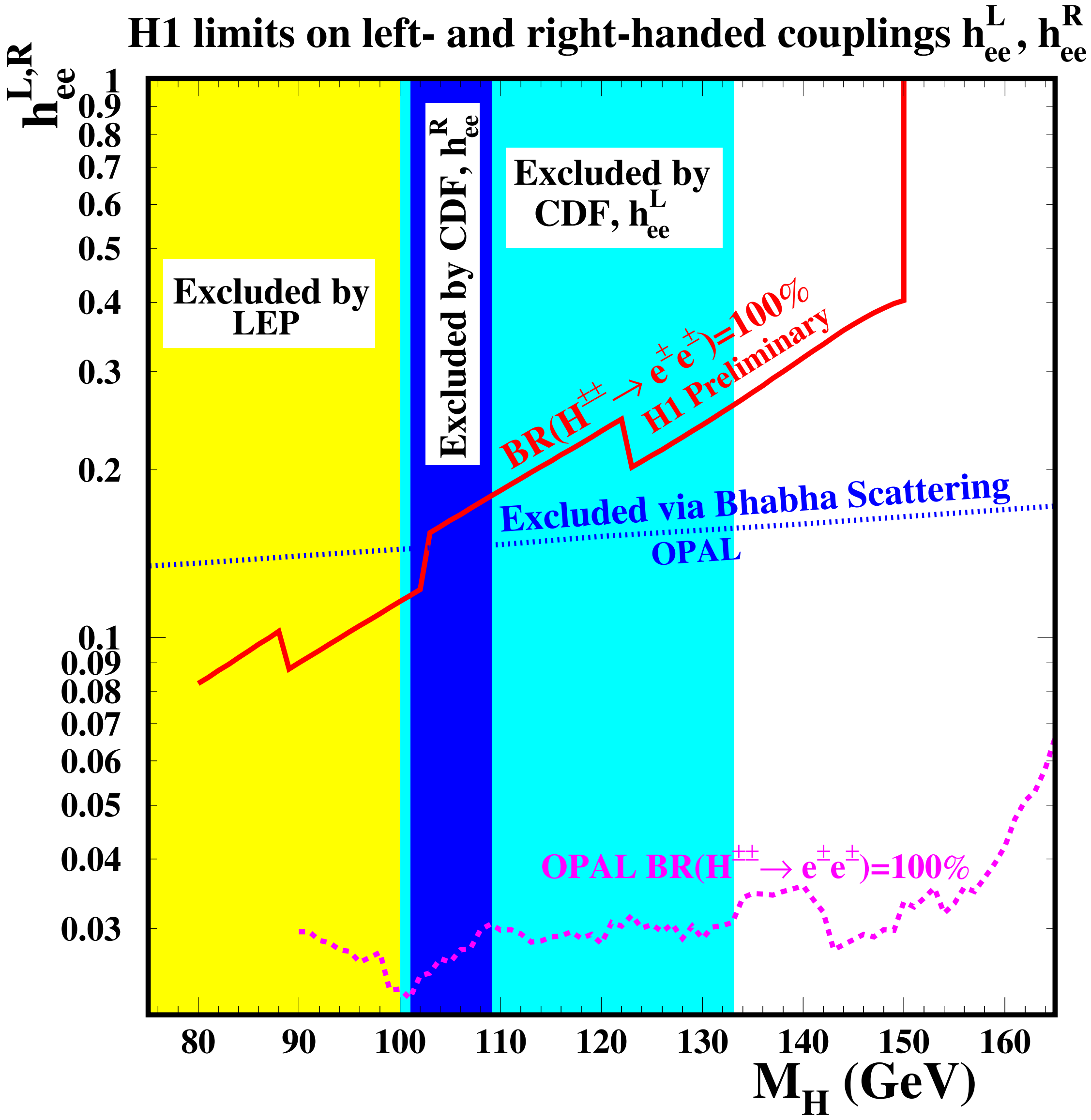

Figure 5: Exclusion limits on the coupling $h_{ee}^{L,R}$ at 95% confidence level as a function of the doubly-charged Higgs mass for the decay $H^{\pm\pm} \to e^\pm e^\pm$ assuming BR$(H^{\pm\pm} \to e^\pm e^\pm) = 1$. The results of this analysis are compared to indirect limits from Bhabha scattering from OPAL, to limits from direct searches for single production of doubly-charged Higgs from OPAL, and for pair production from the LEP experiments and CDF.

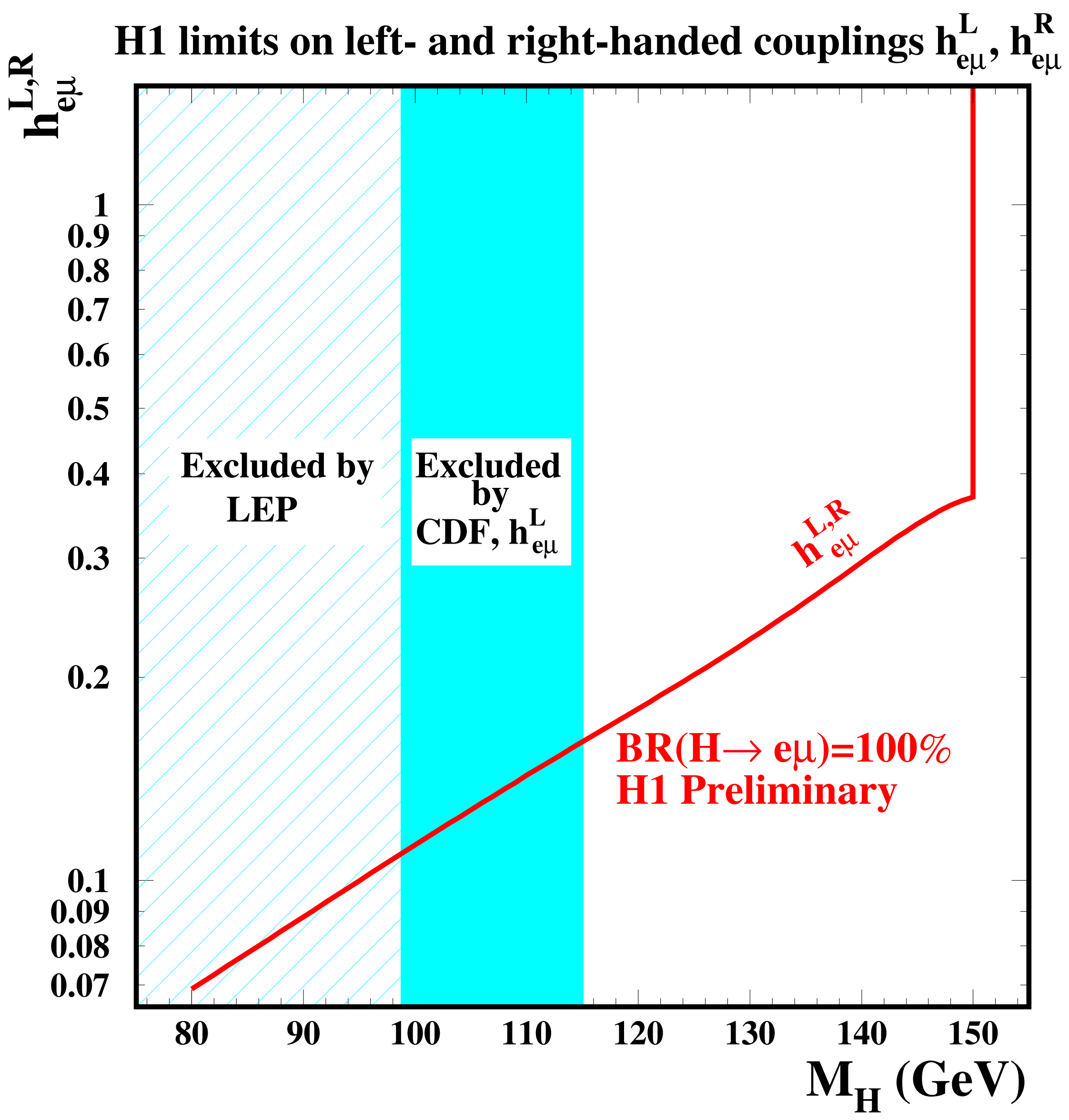

Figure 6: Exclusion limits on the coupling $h^{L,R}_{e\mu}$ at 95% confidence level as a function of the doubly-charged Higgs mass for the decay $H^{\pm\pm} \rightarrow e^{\pm}\mu^{\pm}$ assuming BR$(H^{\pm\pm} \rightarrow e^{\pm}\mu^{\pm}) = 1$. The results of this analysis are compared to limits from direct searches for pair production of doubly-charged Higgs from the LEP experiments and CDF.